

Bio-electrospraying 3-D Organotypic Human Skin Cultures

Vignesh Jayarajan, Jensen O. Auguste, Kenilson A. Gene, Libny Auguste, Camilo Nunez, Bartłomiej Marcinowski, and Suwan N. Jayasinghe*

Organotypic 3D tissue models have greatly contributed to understand a wide range of molecular and cellular characteristics within a functional or diseased tissue. Human skin reconstructs which act as models are most useful for a wide range of investigations, ranging from tissue engineering and regenerative medicine, drug development, screening, and discovery to name a few. There are many approaches for reconstructing 3D skin tissue models, however, to date there have been very few that are able to generate organotypic 3D constructs with a single technology having minimal processing steps to finally scalability. The many manifestations of 3D bioprinting have contributed to this endeavor, having said that, the technology's limitations have tempered those reconstructed models, as they are known to contain low cell numbers/concentrations to those having damaged/dead molecules/cells within the reconstructed tissue, which are not desirable, for exploring as tissues models. Contrary to 3D bioprinting approaches, bio-electrosprays have been demonstrated to possess the ability to handle large concentrations of cells and molecules to whole fertilized embryos without damaging them from a molecular level upwards. Consequently, this article demonstrates, for the first time, bio-electrospray's capacity to reconstruct skin-like structures in vitro and its potential in reconstructing full-thickness 3D organotypic human skin tissues.

1. Introduction

Over the past 30 years or so there have been many approaches explored for the reconstruction of model tissues, useful for studying a wide range basic sciences to their utility in applications ranging from regenerative medicine to drug discovery and delivery to name a few. These studies have recently contributed to the FDA approving human drug trials without the need for animal testing.^[1] There are several platforms for reconstructing 3D tissues, these range from non-jet-based to jet-based approaches. The non-jet-based approaches range from basic manual pipetting, hanging droplet to lithography-based methodologies. Although some tissues have been reconstructed using these methods, these approaches have been found to be tedious and have limitations generating two or more layer/core cellular architectures, especially in the case of the hanging droplet, which in most scenarios have resulted in the constructs giving rise to central necrosis.^[2] Lithography approaches have also been elucidated as having limitations in reconstructing 3D cellularized architectures, these

result from the process damaging the directly handled cells/molecules, arising from the heat by laser exposure (optical tweezers) during the reconstruction process. Additionally, the photo resins explored are cariogenic to both biomolecules and cells, used for cross-linking/hardening the areas/surfaces exposed to the light/lasers.^[3] Therefore, these approaches are tempered as a result of their operational characteristics and capabilities. In the case of jet-based approaches, 3D bioprinting, microfluidics, bio-electrospraying (BES), and aerodynamically assisted bio-jetting (AABJ), have contributed significantly to this endeavor. Although 3D bioprinting in its many manifestations (piezoelectric, solenoid, to extrusion driven), has contributed to this arena, the technology has inherent restrictions, which have risen as the technology inflicts shear stresses within the jetting needles resulting in molecular and cellular damage/death during the printing process.^[3,4] Microfluidics, a technology (flow-driven channel technology) capable of generating highly controlled single and multicore architectures, similar in some respects to 3D bioprinting is incapable of handling large concentrations of cells, thus limiting the processable cell numbers and scaling up of the reconstruction of tissues.^[5] Contrary to both these jetting approaches, bio-electrospraying and aerodynamically

V. Jayarajan

Infection, Immunity, and Inflammation Research & Teaching Department
UCL Great Ormond Street Institute of Child Health
30 Guilford Street, London WC1N 1EH, UK

J. O. Auguste, K. A. Gene, L. Auguste, C. Nunez, B. Marcinowski

Universal BioProducts

2151 South 30th Street, Haines City, FL 33844, USA

S. N. Jayasinghe

BioPhysics Group

Institute of Biomedical Engineering


Centre for Stem Cells and Regenerative Medicine

and Department of Mechanical Engineering

University College London

Torrington, London WC1E 7JE, UK

E-mail: s.jayasinghe@ucl.ac.uk

 The ORCID identification number(s) for the author(s) of this article can be found under <https://doi.org/10.1002/small.202304940>

© 2023 The Authors. Small published by Wiley-VCH GmbH. This is an open access article under the terms of the Creative Commons Attribution License, which permits use, distribution and reproduction in any medium, provided the original work is properly cited.

DOI: 10.1002/small.202304940

Table 1. Measured properties of phosphate buffer saline (PBS) and the explored cell suspensions.

Material	Viscosity [mPa s]	Electrical conductivity [S m ⁻¹]	Surface tension [mN m ⁻¹]	Relative permittivity	Density [kg m ⁻³]
PBS	≈1.05	1.4	68.3	≈77	≈1.12
Fibroblasts 2 × 10 ⁶ cells mL ⁻¹ in hydrogel	≈0.98	≈1.0	≈71	≈70	≈1100
Keratinocytes 2 × 10 ⁶ cells mL ⁻¹ in complete media	≈0.89	≈1.3	≈70	≈68	≈1181
Fibroblasts 1 × 10 ⁵ cells mL ⁻¹ in hydrogel	≈1.0	≈0.9	≈70	≈69	≈925
Keratinocytes 5 × 10 ⁵ cells mL ⁻¹ in complete media	≈0.90	≈1.2	≈71	≈70	≈859

assisted bio-jetting, explore large inner bore needles (>1000 μm) which significantly reduce shear stresses. In fact, both these technologies have been demonstrated for the direct handling of cell suspensions containing single and multiple living cells and/or molecules, to whole fertilized organisms. Thus, demonstrating their significance to human healthcare (and to many other fields of research and development), and flexibility for the handling of the most complex and sensitive materials known to humankind.^[6] Additionally, unlike 3D bioprinting and microfluidics, bio-electrosprays and aerodynamically assisted bio-jetting are able to generate cell bearing droplets far smaller (droplets and residues in the few μm) than the diameter of the needle used. The reader should note that although these technologies use larger inner bore needles, their driving mechanisms are different, namely bio-electrosprays operate over an electric field, while aerodynamically assisted bio-jetting is driven via a pressure gradient. Interestingly both these technologies can be scaled up with ease. However, in this article the authors will focus on bio-electrosprays.

Briefly, bio-electrosprays^[7] work on the principal of applying a high voltage to a conducting needle holding the flow of a cell suspension, relative to a grounded electrode placed inline and below the exit of the charged needle. The flowing cell suspension in the needle is charged, and as it exits the needle and enters the electric field, transforms the exiting cell suspension into a liquid cone from which a liquid jet is seen to emanate from the apex of the cone, subsequently breaking down into a 3D conical spray plume or stream of cell-bearing droplets. This approach has been explored for handling a wide range of human and animal cells (primary, immortalized, and stem cells) and whole fertilized organisms which have been shown to be indistinguishable from those controls, post-exposure.^[6,7] Our previous work with bio-electrosprays have also demonstrated the ability to use this platform biotechnology for reconstructing 3D human tuberculosis models.^[8] Therefore, in this article we extend the application of bio-electrosprays for the reconstruction of organotypic 3D human skin cultures. The authors see the potential of these organotypic model/cultures which could be used for studying a wide range of skin diseases to the use of such diseased/healthy models for testing drugs to other exotic compounds for understanding basic molecular and cellular mechanisms to their

use for developing and discovering new and personalised drugs.

2. Results and Discussion

Initially the hydrogel as supplied was thawed as per the manufacturer protocol and mixed in with human fibroblasts (HFs) at a concentration of 2 × 10⁶ cells per mL⁻¹ using manual pipetting. Prior to seeding the cell suspension, it was assessed for its properties namely, viscosity, electrical conductivity, surface tension, density, and relative permittivity. These five properties alongside the electric field between the electrodes and the flow rate have been known to have effect on the spraying process, in particular, jet formation and its stability during spraying. The equipment used for measuring viscosity, electrical conductivity, surface tension, density, and relative permittivity was calibrated with phosphate buffer saline (PBS) prior to the cell suspension properties being measured. Repeated measurements for each property were recorded. **Table 1** lists the measured values for each property for PBS and four prepared cell suspensions at different cell concentrations. Six fresh samples were subsequently created at a concentration of 2 × 10⁶ cells per mL⁻¹ and split into two categories, namely controls, which were manually seeded, while the remaining three were bio-electrosprayed. Briefly, bio-electrospraying was carried out with the ring ground electrode configuration (**Figure 1**). For seeding, a 6-well plate was used to place six rings (electrodes) manufactured from surgical steel having an internal and outer diameter of ≈1.3 and ≈1.9 cm respectively, with a height of ≈1 cm. One end of the ring was flat while the other was chamfered at approximately 45°. The chamfered side faced the base of each well. The function of these rings was twofold, namely, to contain the manually and bio-electrospray (as a grounded electrode) seeded cells in a confined space, within the well yet allowing, once seeded the construct to have access to nutrients during culture/incubation. The bio-electrospraying process was captured using a high-speed digital camera system which demonstrated, spraying taking place in an unstable jetting mode (**Figure 2a**). This jetting behavior is not unexpected as the measured suspension properties (**Table 1**) have previously been known to generate instability,^[7] with the electrical conductivity and viscosity being high and low respectively. Achieving

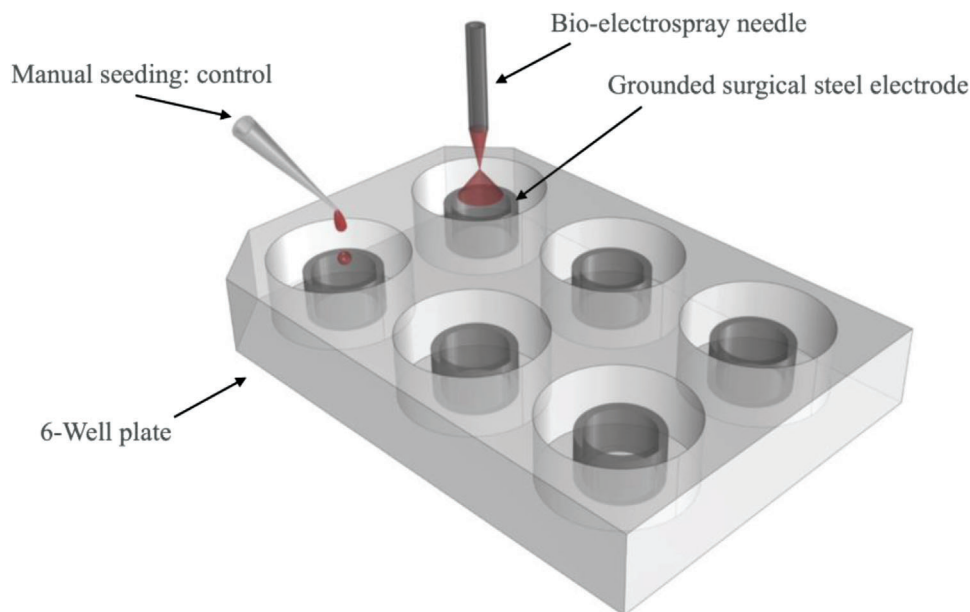


Figure 1. Drawing showing the manual and bio-electrospray seeding process.

stability in the spraying of such a cell suspension can be accomplished as we have previously done so, using the addition of biomolecules/cell compatible polymer solutions which increase the viscosity of the cell suspension, to the exploration of a coaxial needle configuration.^[9] In these investigative studies, spraying stability was not tackled as the primary goal was to assess if bio-electrosprays were capable of constructing a 3D organotypic skin culture/model.

For bio-electrospraying the equipment was setup so that the needle was directly and centrally placed above the surgical ring grounded electrode (Figure 1). The electrical field was set to 0.5 kv mm^{-1} over a distance of 10 mm and spraying was carried out into the three remaining grounded surgical steel rings. The samples were subsequently incubated at 37°C and $10\% \text{ CO}_2$ over 24 h. Post-incubated samples were exposed to seeding of hu-

man keratinocytes (HKs) at a concentration of $2 \times 10^6 \text{ cells mL}^{-1}$ using manual and bio-electrospraying to the two sample categories, respectively. The bio-electrospraying of keratinocytes was also seen to follow the same mode of jetting, namely unstable jetting mode (Figure 2b). All samples were reincubated for 72 h. Following the 2nd incubation, the generated samples were lifted and placed on stainless steel micromeshes accommodated in petri dishes holding complete media. These micromeshes were partly submerged in complete media, thus exposing all samples to an air-media interface. After a period of 15 days these samples were cryopreserved and sectioned as described.

Cryosectioning was carried out where each section was at a thickness of $10 \mu\text{m}$. Samples were sectioned and placed on microslides. These samples were later labeled using H&E staining.

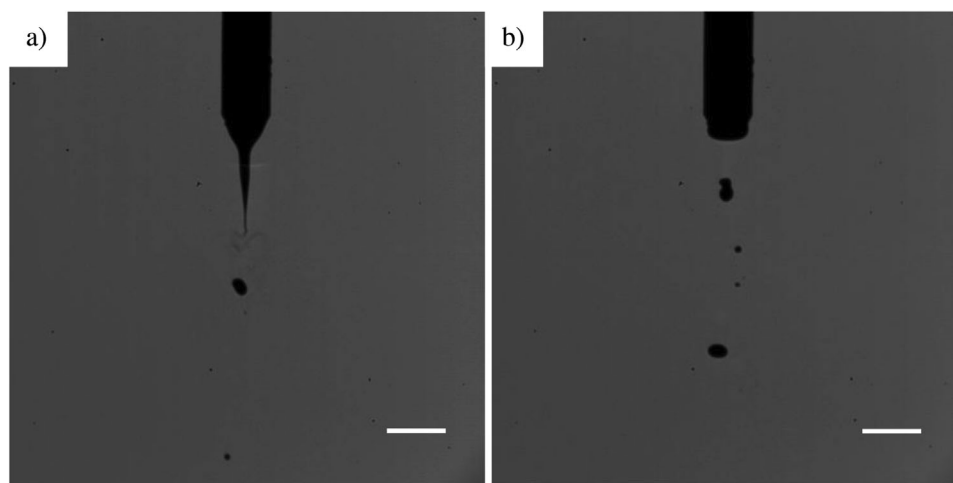


Figure 2. Representative digital high-speed images capturing the bio-electrospraying at a frame rate of $\approx 10\,000 \text{ fps}$ of a) the hydrogel containing the fibroblasts at a cell concentration of $2 \times 10^5 \text{ cells mL}^{-1}$, and b) keratinocytes at a cell concentration of $2 \times 10^5 \text{ cells mL}^{-1}$. Scale bar represents $1350 \mu\text{m}$.

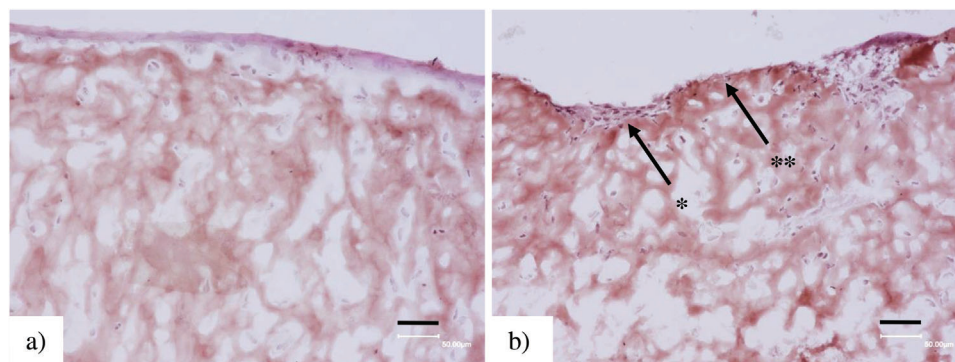


Figure 3. Characteristic bright field microscope images of the cryosectioned a) manually and b) bio-electrosprayed organotypic skin tissues. Note in panel (a) the uniform epidermis and b) the nonuniform epidermis (indicated with arrows). In panel (b) the epidermis varies in thickness over the troughs (*) and crests (**). Scale bar in both panels represents 50 μm .

The stained sections were analyzed using bright field microscopy (Figure 3).

Bright field microscopy demonstrated those manually seeded constructs having an epidermis thickness of approximately 30 μm and a dermis of over 300 μm (Figure 3a). Moreover, in those bio-electrosprayed constructs it was noticed the formed epidermis had an inconsistent thickness over the entire construct, which seemed to have an undulated profile, with troughs and crests (Figure 3b). On measuring the width of each trough containing a thicker epidermis (Figure 3b), we noticed this corresponded well with the diameters of the larger keratinocyte bearing droplets generated via the bio-electrosprays (Figure 2b). Therefore we concluded that these fast moving larger cell bearing droplets, on impact with the soft hydrogel were able to create troughs, thus forming a nonuniform epidermis over the whole area of the construct. Therefore, we decided to modify the hydrogel protocol and the explored cell concentrations. With regards to the hydrogel the implemented modification in protocol was to allow the fibroblast containing hydrogel at least 72 h culturing, in an incubated before exposing to the keratinocytes. Thus allowing the hydrogel time to gel to a greater stiffness. This together with the reduction in cell concentration, would effectively reduce the density of each cell containing droplet (having less cells within a droplet) impacting and impinging the fibroblast accommodating hydrogel. Therefore, reducing droplet driven surface impingement on the hydrogel and on its overall surface profile.

With these modifications to the hydrogel protocol and the cell concentrations, we repeated the experiments following the previous steps, but this time around manually seeding and bio-electrospraying fibroblasts at a concentration of 1×10^5 cells mL^{-1} . Post-seeding the samples were incubated for over 72 h at 37 $^{\circ}\text{C}$ and 10% CO_2 . Keratinocytes on this occasion were seeded at a concentration of 5×10^5 cells mL^{-1} either manually or bio-electrospraying to the respective wells and incubated for over 14 days. Interestingly we noticed the reduction in cell concentration had a significant effect on the spraying mode. High-speed images captured the spraying of both the hydrogel containing fibroblasts and keratinocytes in completed media, taking place in the unstable spindle mode (Figure 4). Most notably it was observed through the captured images that spraying took place without the formation of large cell-bearing droplets as observed with the high concentrated cell suspensions (Figure 2). From our

previous experience with bio-electrosprays, smaller cell-bearing droplets result from a combination of surface tension effects and low cell density suspensions, which reduce cell clustering while in suspension and within the cone, promoted by the stagnation zone.^[10] Additionally, the spray mode is also affected by reducing the suspension cell concentration, as the predominant material is the liquid, in this case the complete media.

On day 14 the samples were lifted and exposed to an air–liquid interface using the micromeshes submerged in complete media. These samples were cryopreserved as described, cryosectioned and subsequently stained as previously carried out. Bright field microscopy on these sections which were at a thickness of 10 μm are seen in Figure 5a,b. Immunofluorescence staining shown in Figure 5c and d demonstrates that keratinocytes having arranged themselves as layers within both the generated skin cultures, respectively. Note that the nuclear staining labels all nuclei (blue) of both cell types (fibroblasts and keratinocytes), whereas keratinocytes were distinguished from fibroblasts using pan-keratin antibody staining that is very specific for keratinocytes. These experimental modifications we made were seen to have significant effects on the generated constructs, namely in this case the constructs were comparable. The increased incubation together with the lower concentrated fibroblasts suspensions seem to allow the construct to have maintained its integrity postexposure to the bio-electrospraying of the lower concentrated keratinocyte suspensions. Thus, enabling the formation of a near uniform epidermis over the entire construct and comparable with those epidermizes formed in the manual seeding. Interestingly even the manually seeded constructs at these experimental conditions seem to have generated a thicker epidermis although a lesser cell concentration was used. This re-enforced our decision to allow the hydrogel to stabilize, while cell maturation also took place, with a lower cell concentration before it was exposed to the keratinocytes.

3D-skin equivalent cultures are generally presented with distinct epidermal layers, from basal layer to cornified layer at the top. However, it is important to note that Jayarajan et al., used de-epidermalized dermis as a base for generating such matured cultures *in vitro*.^[11] Rather, the main focus of this study was to elucidate the compatibility and feasibility of bio-electrospraying human primary fibroblasts in combination with a collagen hydrogel and subsequently keratinocytes in complete media, but not on de-epidermalized dermis.

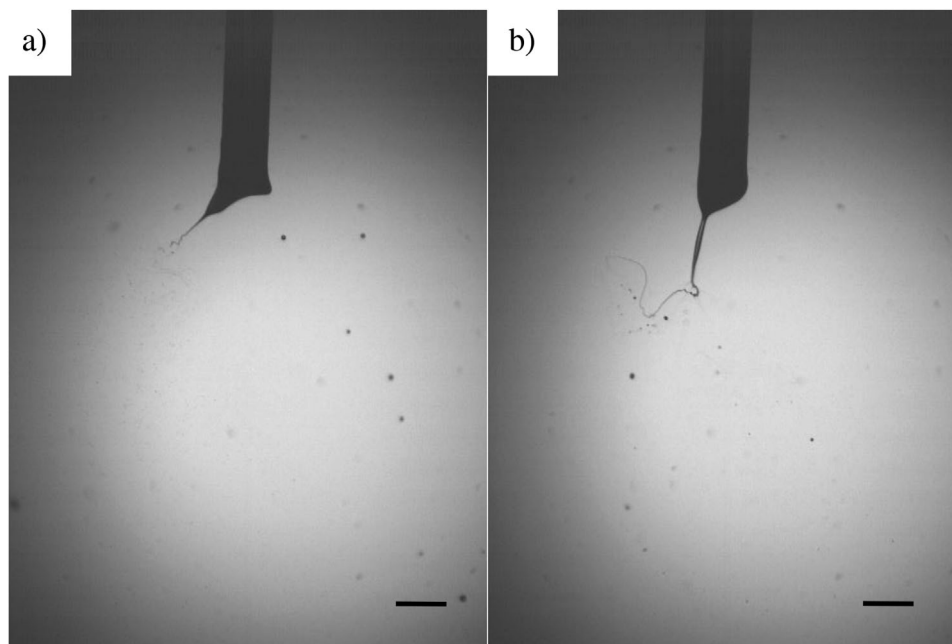


Figure 4. High-speed images of the bio-electrospraying process captured at $\approx 10\,000$ fps of a) the hydrogel containing fibroblasts at a concentration of 1×10^5 cells mL^{-1} and b) keratinocytes suspended at a concentration of 5×10^5 cells mL^{-1} in complete media. Scale bar represents $1350\ \mu\text{m}$.

Interestingly the versatility and flexibility of bio-electrosprays allowed no limitations in the direct handling of suspensions containing either high or lower cell densities. Although in this scenario a lower cell concentration was desirable to reconstruct an organotypic skin tissue/model.

3. Conclusion

In these investigative studies we demonstrate bio-electrospray's capacity to reconstruct human skin tissue/models. The protocols used for generating these constructs required some minor modifications, which resulted in tissues that were comparable to those generated through manual seeding. We hope to further these studies in the future, where we wish to investigate the exploration of more significantly modified hydrogels, containing more additives in terms of concentrations of collagen and others such as laminin, to the use of human derived hydrogels. Similar results were achieved with cell electrospinning. These investigations provide the impetus to pursue this bioplatfrom for reconstructing full think skin tissues, which we hope to test a wide range of aspects at the molecular, cellular to the physiological levels.

4. Experimental Section

Bio-electrospray Equipment and Setup: The bio-electrospray equipment setup explored in these studies employed a ring ground electrode. The ring used in these studies were not only used to attract the charged droplets toward it but was also used as a collection ring which restricted the droplets collected to only within the ring. Thus, the collected cell-bearing droplets within the inner ring, postjetting would take the shape of the inner ring on gelation at ambient temperature. The applied voltage (FP-30, Glassman Europe Ltd, Tadley, UK) and flow rate (PHD 4400, HARVARD Appa-

ratus Ltd, Edenbridge, UK) were varied over a wide range. This variation was systematically carried out with the change in the distance between the two electrodes. All aspects were optimized for these cells and hydrogel containing cell suspensions. The bio-electrospray needle used in these studies had an internal and external diameter of ≈ 900 and $\approx 1350\ \mu\text{m}$ respectively. Bio-electrospraying was carried out in a laminar flow safety cabinet.

Cell Culture: Primary HKs and donor-matched primary HFs between passage 1 and 3 (HKs), and passage 4 and 6 (HFs) were used in this study. HKs were cultured as previously described.^[11] Briefly, HKs were cultivated in a humidified atmosphere at $37\ ^\circ\text{C}$ with $10\% \text{CO}_2$ in Green's medium containing DMEM and DMEM/F12 in the ratio of 1:1 supplemented with $10\% \text{FCS}$ (Labtech, Heathfield, UK, # FCS-SA), $50\ \text{U mL}^{-1}$ penicillin and streptomycin (Gibco, Paisley, UK, # 15 070 063), $10\ \text{ng mL}^{-1}$ EGF (Peprotech, London, UK, # AF-100-15-1000), $0.4\ \mu\text{g mL}^{-1}$ Hydrocortisone (Sigma, Gillingham, UK, # H-2270), $5\ \mu\text{g mL}^{-1}$ Transferrin (Sigma, # T2252), $5\ \mu\text{g mL}^{-1}$ Insulin (Sigma, # I-5500), $2 \times 10^{-11}\ \text{M}$ Liothyronine sodium salt (Sigma, # T6397), and $1 \times 10^{-10}\ \text{M}$ Cholera toxin (Sigma, # C-8052). keratinocytes were passaged and reseeded at a density of $1.5 \times 10^4\ \text{cm}^{-2}$. HKs were cocultivated with i3T3 at a density of $3 \times 10^4\ \text{cm}^{-2}$ unless specified. Whereas HFs were cultivated in a humidified atmosphere at $37\ ^\circ\text{C}$ with $10\% \text{CO}_2$ in DMEM supplemented with $10\% \text{FCS}$ (Labtech) and $50\ \text{U mL}^{-1}$ penicillin and streptomycin (Gibco, UK).

Hydrogel and Measuring Cell Suspensions Properties: The collagel hydrogel (ACGH-002) explored in these investigative studies, was a biocompatible complex of type I collagen fibers and ECM mixture, supporting the cell/3D tissue culture. This hydrogel contains high-quality, sterile type I tendon collagen which has been specially formulated for ease of gel formation. Once in a 3D tissue model, the collagel hydrogel would not break or tear apart easily when stretched. This collagel ydrogel was free flowing, allowing it to be readily used for mixing with cells for bio-electrospraying.

The conductivity of all the suspensions explored in these studies were measured using an RS PRO conductivity meter. The meter was calibrated with a fresh solution of PBS, subsequently the prepared suspensions were measured. Similar to measuring conductivity, the equipment used for measuring the properties, viscosity, surface tension, density, and relative permittivity were all calibrated with fresh samples of PBS. Viscosity was measured using a Haake RS150 cone and plate rheometer, surface

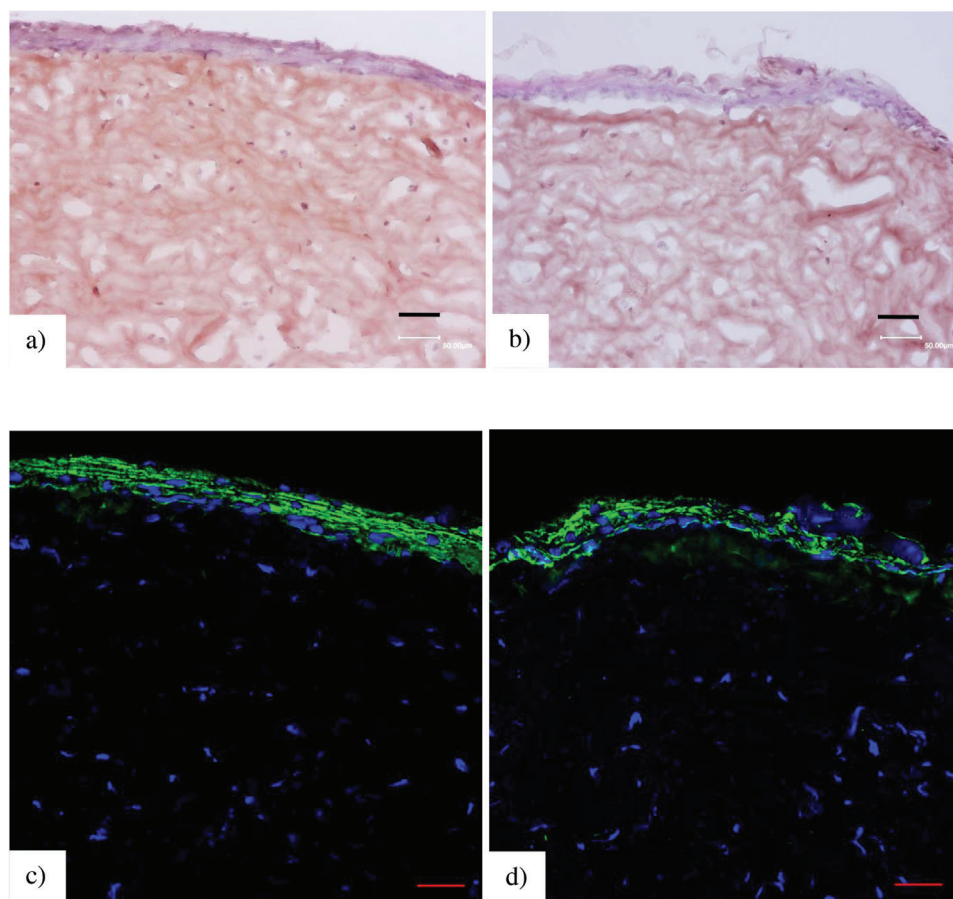


Figure 5. Representative bright field and fluorescent microscope images of the sectioned a,c) manually and b,d) bio-electrosprayed organotypic skin cultures respectively. It is evident that allowing the cell-bearing hydrogel to stabilize (increased its stiffness) through longer incubation periods with a lower concentration of cell loading to subsequently exposing a lower concentrated keratinocyte suspensions addressed the uneven epidermis formed. c,d) Demonstrates through fluorescent staining, the keratinocytes arranged as layers within the epidermis, as expected and comparable, to those found in the epidermis in the manually seeded cultures. Scale bar in all panels represent 50 μm .

tension was via a Du Novy balance and the ring separation method. Density was measured using a density bottle and finally the relative permittivity was measured using a permittivity cell. The permittivity cell used in these studies had two copper plates of known area (A) and maintained at a distance of ≈ 36 mm. The samples were inserted between the plates and capacitance (C) was measured, taking the permittivity of free space to be ϵ_0 as 8.854×10^{-12} F m^{-1} , relative permittivity values, were calculated as Cd/ϵ_0A . Table 1 lists all the measured values for the properties of the media and cell suspensions explored in these studies.

Cryosectioning: Manually and bio-electrosprayed reconstructs at day 15 were instantly frozen after embedding in optimal cutting temperature compound (Tissue-Tek, Belgium, #94-4583), and stored at -70 °C for cryosectioning. Consequently these frozen constructs were cut into 10 μm slices at -20 °C using a Leica CM1850 Cryostat (Leica Instruments, UK) and transferred onto polylysine adhesion slides (Thermo Fisher Scientific, UK, # 10219280). Slides were later stained.

Hematoxylin and Eosin Staining: Air-dried sections were rinsed with water, hematoxylin (Gill no. 3, Sigma, #GHS332) was added on the sections for 40 min. Slides were then rinsed with water and dipped in 2% HCL in 70% ethanol once to induce hematoxylin differentiation. Slides were further rinsed with hot tap water, immersed in Scott's tap water for 1 min and rinsed with hot tap water again before incubating with 1% eosin (Sigma, #HT110232) for 2 min. Slides were then dehydrated by dipping in tap water, 70%, and 100% ethanol for 30 s each. Dehydrated sections were cleared by dipping in xylene for 30 s. Slides were finally dried and mounted

using DPX new (Sigma, #100579). The stained sections were examined using a Keyence VHX 7100 microscope.

Fluorescent Staining and Imaging: The frozen sections were allowed to dry naturally at room temperature for 30 min and subsequently rinsed with PBS for 5 min. Afterward, the sections were treated with a blocking solution of 3% FCS in PBS, followed by overnight incubation with the primary anti pan-Keratin antibody (neat, in-house clone LP34) at 4 °C. The next day, the slides were washed three times with PBS, each for 5 min, and then incubated with anti-mouse Alexa Fluor Plus 488 antibody at room temperature for 1 h. Subsequently, the slides were washed three times for 5 min each and counterstained with Hoechst 33342, which was diluted in a 1:10 000 ratio with PBS, for 5 min. The counterstained sections were washed three times for 5 min each. Finally, the sections were mounted using Fluoromount-G mounting medium from Thermo Fisher Scientific (# 00-4958-02) and examined under a ZEISS LSM710 inverted confocal microscope (Carl Zeiss Ltd, UK).

Acknowledgements

The authors are thankful to Prof. Wei-Li Di, at the Institute of Child Health at UCL, for providing the keratinocytes and fibroblasts explored in these investigations. S.N.J. gratefully acknowledges the seed corn funding provided by the Royal Society in United Kingdom. V.J. was supported by Newlife – the Charity For Disabled Children.

Conflict of Interest

The authors declare no conflict of interest.

Data Availability Statement

The data that support the findings of this study are available from the corresponding author upon reasonable request.

Keywords

additive biomanufacturing, bio-electrosprays, biological models, organotypic 3D human skin tissue, skin cultures, cells

Received: June 12, 2023

Revised: August 16, 2023

Published online:

-
- [1] M. Wadman, *Science* **2023**, 379, 127.
[2] S. E. J. Han, S. Kwon, K. S. Kim, *Cancer Cell Int.* **2021**, 21, 152.
[3] H. E.-Q. Xu, J.-C. Liu, Z.-Y. Zhang, C.-X. Xu, *Med* **2022**, 9, 70.

- [4] a) G. M. Nishioka, A. A. Markey, C. K. Holloway, *J. Am. Chem. Soc.* **2004**, 126, 16320; b) L. Ning, N. Betancourt, D. J. Schreyer, X. Chen, *ACS Biomater. Sci. Eng.* **2018**, 4, 3906.
[5] a) T. Suwannaphan, A. Pimpin, W. Srituravanich, W. Jeamsaksiri, W. Sripumkhai, D. Ketpun, A. Sailasuta, P. Piyaviriyakul, presented at 8th Biomedical Engineering International Conference (BMEiCON), Pattaya, Thailand, November **2015**, p. 1; b) Y. B. Bae, H. K. Jang, T. H. Shin, G. Phukan, T. T. Tran, G. Lee, W. R. Hwang, J. U. M. Kim, *Lab Chip* **2016**, 16, 96.
[6] a) S. N. Jayasinghe, *Analyst* **2011**, 136, 878; b) P. Joly, N. Chavda, A. Eddaoudi, S. N. Jayasinghe, *Biomicrofluidics* **2010**, 4, 011101; c) N. K. Pakes, S. N. Jayasinghe, R. S. B. Williams, *J. R. Soc., Interface* **2011**, 8, 1185.
[7] S. N. Jayasinghe, A. N. Qureshi, P. A. M. Eagles, *Small* **2006**, 2, 216.
[8] a) V. L. Workman, L. B. Tezera, P. T. Elkington, S. N. Jayasinghe, *Adv. Funct. Mater.* **2014**, 24, 2648; b) L. B. Tezera, M. K. Bielecka, P. Ogongo, N. F. Walker, M. Ellis, D. J. Garay-Baquero, K. Thomas, M. T. Reichmann, D. A. Johnston, K. A. Wilkinson, M. Ahmed, S. Jogai, S. N. Jayasinghe, R. J. Wilkinson, S. Mansour, G. J. Thomas, C. H. Ottensmeier, A. Leslie, P. T. Elkington, *Elife* **2020**, 9, 52668.
[9] a) H. C. O'Neill, W. E. Maalouf, J. C. Harper, S. N. Jayasinghe, *Mater. Today* **2019**, 31, 21; b) S. N. Jayasinghe, A. Townsend-Nicholson, *Lab Chip* **2006**, 6, 1086.
[10] I. Hayati, A. I. Bailey, T. F. Tadros, *Nature* **1986**, 319, 41.
[11] V. Jayarajan, G. T. Hall, T. Xenakis, N. Bulstrode, D. Moulding, S. Castellano, W.-L. Di, *Cells* **2023**, 12, 346.